Med Chem Res (2014) 23:2584–2595
DOI 10.1007/s00044-013-0854-3

MEDICINAL CHEMISTRY RESEARCH

ORIGINAL RESEARCH

Synthesis and antitumor properties of novel curcumin analogs

Hui Luo · Shengjie Yang · Qi Zhao · Hongmei Xiang

Received: 22 July 2013 / Accepted: 15 October 2013 / Published online: 26 October 2013

Abstract A series of novel curcumin (CC) analogs were synthesized by reacting substituted aldehydes with intermediates **4a** and **4b**. The inhibitory activities of these CC analogs were investigated on human cancer cells PC3, Bcap-37, and MGC-803 in vitro by MTT assay. The results showed that most of the title compounds displayed moderate to high levels of antitumor activities. Compound **5f**, the most active CC analogs, has the IC_{50} values of 1.34 ± 0.28, 3.90 ± 0.36, and 0.86 ± 0.44 μM against the three human cancer cells assayed, respectively. Furthermore, subsequent fluorescence staining and flow cytometry analysis indicated compound **5f** could induce apoptosis in PC3, Bcap-37, and MGC-803 cells, and the apoptosis ratio reachs the peak (27.1 %) in MGC-803 cells at 24 h after treatment at 10 μM.

Keywords Curcumin analogs · Antitumor · Apoptosis · Flow cytometry analysis

Abbreviations

ADM	Adriamycin
AO/EB	Acridine orange/ethidium bromide
CC	Curcumin
^{13}C NMR	^{13}C nuclear magnetic resonance
DMSO	Dimethyl sulfoxide
FCM	Flow cytometry
HCPT	10-Hydroxyl camptothecine
^{1}H NMR	Proton nuclear magnetic resonance
IR	Infra-red
MTT	3-(4,5-Dimethylthiazol-2-yl)-2, 5-diphenyltetrazolium bromide

Introduction

Curcumin (CC) is the principal curcuminoid of the popular Indian spice turmeric, which is a member of the ginger family (Zingiberaceae) (Archana *et al*., 2011; Khanna *et al*., 2009). CC and its derivatives have been revealed having antitumor (Wilken *et al*., 2011; Sa and Das, 2008), antioxidant (Menon and Sudheer, 2007; Jayaprakasha *et al*., 2006), antiarthritic (Zahidah *et al*., 2012), antiamyloid (Ringman *et al*. 2005), anti-ischemic (Shukla *et al*., 2008), and anti-inflammatory (Menon and Sudheer, 2007; Chainani-Wu, 2003) properties in both in vitro and animal studies. They are particularly known for their ability to resist mutation and raise antitumor activity (Lee *et al*., 2011). Their potential anticancer effects stem from an ability to induce apoptosis in cancer cells without cytotoxic

Hui Luo and Shengjie Yang have contributed equally to this study.

H. Luo
Guizhou Fruit Institute, Guizhou Academy of Agricultural Sciences, Guiyang 550006, People's Republic of China

S. Yang
Research Institute of Traditional Chinese Medicine, Yangtze River Pharmaceutical Group Co., Ltd, Taizhou 225321, People's Republic of China

H. Luo · S. Yang · Q. Zhao · H. Xiang
State Key Laboratory Breeding Base of Green Pesticide and Agricultural Bioengineering, Key Laboratory of Green Pesticide and Agricultural Bioengineering, Ministry of Education, Guizhou University, Guiyang 550025, People's Republic of China

H. Luo (✉) · S. Yang · Q. Zhao · H. Xiang
Ctr for R&D of Fine Chemicals, Guizhou University, Huaxi St, Guiyang 550025, People's Republic of China
e-mail: luohui8732@163.com

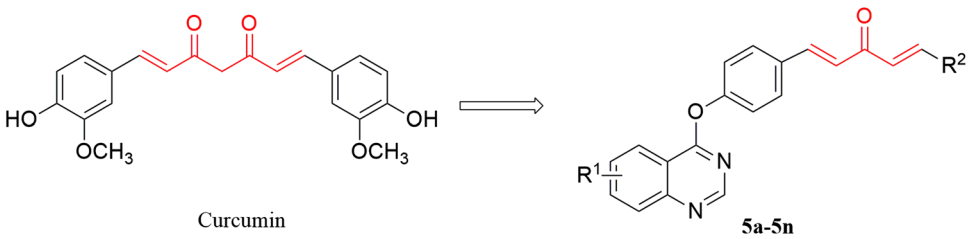

Fig. 1 Design of the target compounds

effects on healthy cells (Ravindran *et al*., 2009; Almanaa *et al*., 2012). Researchers have demonstrated that CC interfered with activity of the transcription factor NF-κB, which had been linked to a number of diseases such as cancer (Lin and Lin, 2008; Kohli *et al*., 2005). In Senft *et al*. (2010) reported that CC could inhibit tumor cell proliferation, migration, and invasion which were mediated through interference with a signaling pathway (Senft *et al*., 2010). In addition, some studies indicated that CC had phytoestrogenic activity that might affect onset of breast cancer (Bachmeier *et al*., 2010). However, the potential use of CC as a therapeutic agent was severely affected by its low water solubility, poor ex vivo bioavailability, and rapid metabolism. Thus, great interest has been devoted to the synthesis of novel CC analogs exhibiting enhanced biologic properties, e.g., the novel ferrocenyl curcuminoids were synthesized by covalent anchorage of three different ferrocenyl ligands. Shibata *et al.* reported some newly synthesized CC analogs containing methoxymethyl group showed unexpected improvements in the anticolorectal cancer activities in vivo (Shibata *et al*., 2009), whereas Yamakoshi *et al.* obtained similar class of compounds by studying structure–activity relationship of C5-curcuminoids **Ai–ii** (Yamakoshi *et al*., 2010). Our group reported several newly synthesized CC analogs showed obvious antitumor activities (Yuan *et al*., 2011). In present work, quinazoline groups were introduced into CC analogs, and sixteen CC analogs were synthesized (Fig. 1). These CC analogs were evaluated their antitumor activities against PC3, Bcap-37, and MGC-803 human cancer cell lines by MTT assay, and were studied their preliminary mechanism by AO/EB staining, Hoechst 33258 staining, DNA Ladder, and flow cytometry analysis.

Results and discussion

Chemistry

Target compounds **5a–5n** were synthesized by reacting the substituted aldehydes with intermediates **4a**, **4b** in EtOH at room temperature, as shown in Fig. 2. Starting from acetone and salicylaldehyde, acetone was excessive and was stirred in sodium hydroxide (1 %) at room temperature to obtain intermediates 4-(4-hydroxy-phenyl)-3-butylene-2-one (**3**). *o*-Aminobenzoic acid was reacted with formamide, and the reaction was maintained for 4.5 h at 140–145 °C to obtain intermediate (**1**). Intermediate (**1**), $SOCl_2$ was added in DMF, and the mixture was refluxed to obtain 4-chloroquine quinazolin (**2**) (reactive intermediate). Intermediates (**2**), and 4-(4-hydroxy-phenyl)-3-butylene-2-one (**3**) were reacted with K_2CO_3 for 3.5 h at 30–40 °C. The crude products were recrystallized from anhydrous alcohol to get intermediates **4a** and **4b** with 76.8 and 80.6 % yields, respectively. The structures of these compounds were confirmed by elements analysis, IR, ^{1}H NMR, and ^{13}C NMR.

Biologic activity

The in vitro antitumor activities of these newly synthesized compounds were evaluated against human prostate cancer cell line PC3, breast cancer cell line Bcap-37, and gastric cancer cell line MGC-803 by 3-(4,5-dimethylthiazol-2-yl)-2,5-diphenyl-tetrazolium bromide (MTT) cell proliferation assay. Adriamycin (ADM) and the compounds were dissolved in DMSO. The negative control cells were treated with culture medium containing 0.1 % DMSO, while ADM was used as positive control. Each experiment was repeated at least three times. The results were reported in terms of IC_{50} values and summarized in Table 1. From the IC_{50} values, all the tested compounds had good activities on all the selected cell lines, with IC_{50} values ranging from 0.86 to 30.29 μM. Compounds **5a–5n** showed significant antitumor activities, but intermediates **4a** and **4b** exhibited only moderate activities. The variation among the different substitutes on R^1 greatly affected the activities. For example, intermediate **4a** (R^1 was H) presented stronger inhibition than **4b** (R^1 was 8-CH_3). Interestingly, when aromatic aldehydes were introduced to the intermediate **4a** or **4b**, an apparent increase in antitumor activity was found. Compounds **5a–5n** (IC_{50}, <15 μM) showed more promising activity as compared to the intermediates **4a** and **4b**. Compound **5f**, the most active compound, had shown IC_{50} values of 1.34 ± 0.28, 3.90 ± 0.36, and 0.86 ± 0.44 μM on PC3, Bcap-37, and MGC-803 cell lines, respectively. Further experiments indicated that proliferation of these three cancer cells was significantly inhibited by compound

Fig. 2 Synthetic route of **5a–5n**

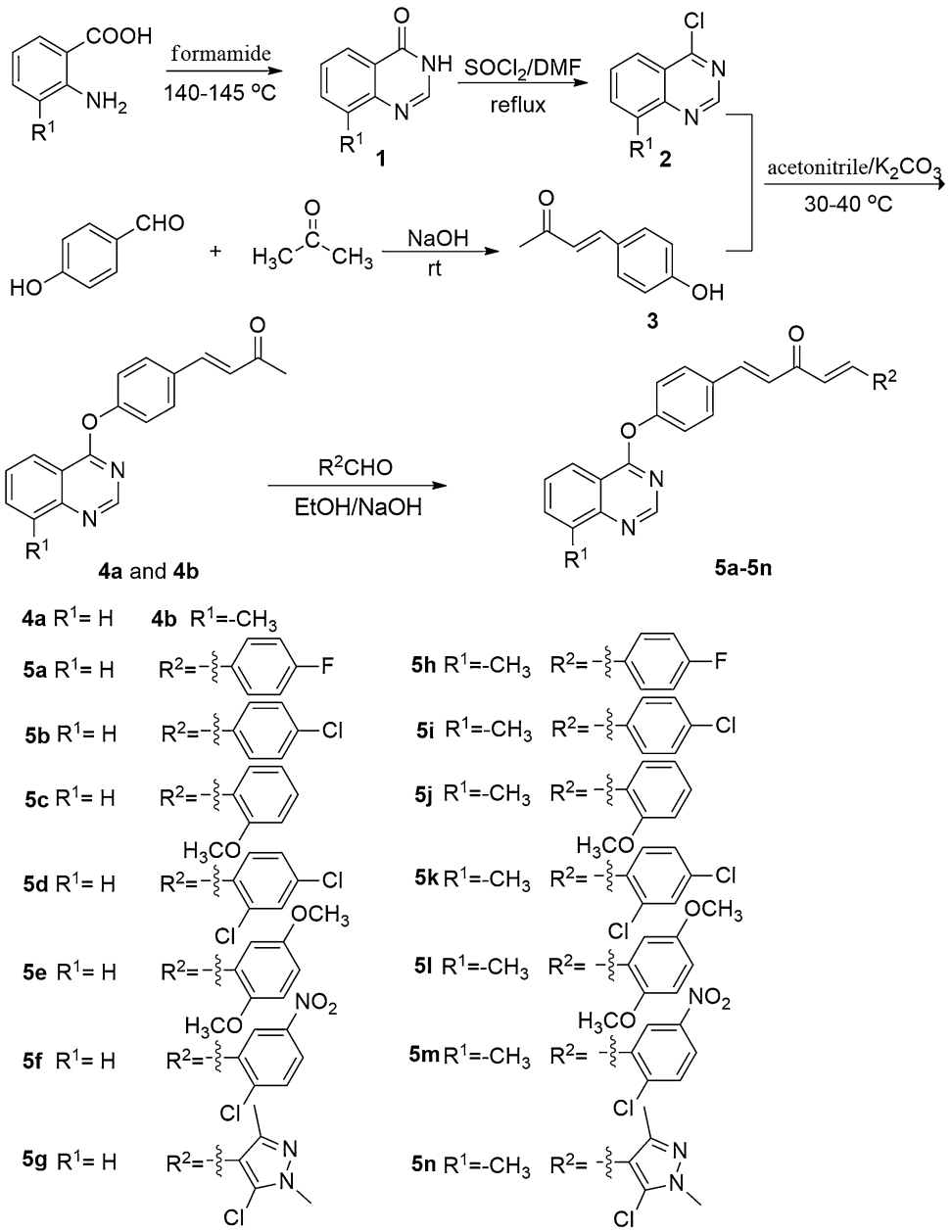

5f in a concentration-dependent manner, as shown in Fig. 3.

In addition, ADM and the active compounds (**5c**, **5e**, and **5f**) were also tested on normal cell line NIH3T3. As shown in Table 2, compound **5f** was less toxic on normal cell line than on cancer cell lines and more selective to cancer cell lines than compounds **5c**, **5e**, and ADM. Thus, compounds **5c**, **5e**, and ADM showed less selective to cancer cells and had some cytotoxic effect on normal cells.

Apoptosis is a physiologic pattern of cell death characterized by morphological features and extensive DNA fragmentation, the frequency, and time of appearance of which depend on the cell line and the apoptosis inducing signal (Wu *et al*., 2012). Thus compound **5f** was selected to analyze the mechanism of growth inhibition of cancer cells. In order to study the preliminary mechanism of action, changes in the morphological character of PC3, Bcap-37, and MGC-803 cells were investigated using acridine orange (AO)/ethidium bromide (EB) staining, Hoechst 33258 staining, and apoptosis-DNA ladder assay to determine compound **5f** whether the growth inhibitory activity was related to the induction of apoptosis. HCPT, which was isolated from a Chinese tree *Camptotheca acuminate*, has a broad spectrum of anticancer activity in vitro and in vivo (Fei *et al*., 2013). It was reported that HCPT could induce apoptosis in human cancer cells (Zhai *et al*., 2010). Therefore, HCPT was used as positive control to study the action mechanism of compound **5f**.

Table 1 The in vitro antitumor activities of compounds **4a**, **4b**, and **5a–5n** against PC3, Bcap-37, and MGC-803 cancer cell lines

Compound	IC_{50} (μM)[a]		
	PC3	Bcap-37	MGC-803
4a	21.31 ± 0.46	28.91 ± 0.52	18.45 ± 0.48
4b	25.79 ± 0.51	30.29 ± 0.46	19.87 ± 0.45
5a	5.62 ± 0.34	8.53 ± 0.46	3.84 ± 0.19
5b	7.35 ± 0.38	11.35 ± 0.42	4.84 ± 0.27
5c	3.66 ± 0.29	7.82 ± 0.26	2.03 ± 0.21
5d	4.57 ± 0.43	10.81 ± 0.58	2.77 ± 0.34
5e	2.96 ± 0.32	7.81 ± 0.29	2.01 ± 0.36
5f	1.34 ± 0.28	3.90 ± 0.36	0.86 ± 0.44
5g	11.52 ± 0.51	18.9 ± 0.44	9.31 ± 0.38
5h	7.36 ± 0.32	9.25 ± 0.50	4.36 ± 0.38
5i	8.79 ± 0.46	12.26 ± 0.32	8.10 ± 0.50
5j	5.17 ± 0.45	9.26 ± 0.41	3.76 ± 0.37
5k	15.24 ± 0.53	32.75 ± 0.56	5.13 ± 0.49
5l	4.71 ± 0.39	8.17 ± 0.38	2.32 ± 0.32
5m	2.79 ± 0.24	7.89 ± 0.53	1.86 ± 0.28
5n	16.42 ± 0.49	21.33 ± 0.41	11.56 ± 0.32
ADM	1.01 ± 0.21	1.90 ± 0.24	0.74 ± 0.18

The data were the mean ± SD obtained from three independent experiments, with ADM used as the positive control

[a] Agent concentration (micromolar) that inhibited cell growth by 50 % 72 h after treatment

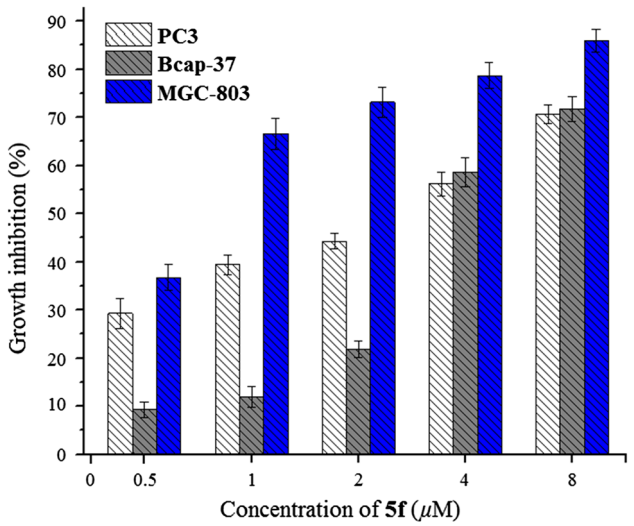

Fig. 3 Effect of **5f** on proliferation of tumor cells. After PC3, Bcap-37, and MGC-803 cells were treated with **5f** for 72 h in the concentration varied from 0.5 to 8 μM. Data are presented as mean ± SD, $n = 4$

The morphologic changes in cells after treatment with compound **5f** were assessed by fluorescence microscopy after staining with AO/EB. Live cells exhibit normal green nuclei early apoptotic cells show bright green nuclei with condensed or fragmented chromatin; late apoptotic cells display condensed and fragmented orange chromatin, whereas necrotic cells showed structurally normal orange nucleus (Kasibhatla *et al*., 2006; Sukardiman *et al*., 2007). The cytotoxicity of compound **5f** at 5 μM against PC3, Bcap-37, and MGC-803 cells for 12 h was detected by AO/EB staining, with HCPT used as a positive control at 10 μM for 12 h.

Table 2 Selectivity index of **5c**, **5e**, and **5f** toward cancer cells

Compound	PC3	Bcap-37	MGC-803
5c	3.40	<2	6.13
5e	4.46	<2	6.57
5f	>8	5.72	>8
ADM	<2	<2	<2

Selectivity index (IC_{50} on mouse embryo fibroblast cell line/IC_{50} on corresponding cancer cell line)

As can be seen in Fig. 4, green yellow or orange dots were detected in the HCPT after 12 h. Yellow and orange dots in PC3, Bcap-37, and MGC-803 cells showed early and late apoptotic cells, and the appearance of little red cells indicated that compound **5f** was associated with low cytotoxicity. The results suggested that compound **5f** was able to induce apoptosis in tumor cells.

Hoechst 33258 staining was also performed to investigate the apoptosis-inducing activities of compound **5f** in PC3, Bcap-37, and MGC-803 cells. Live cells with homogeneous light blue nuclei could be observed under fluorescence microscopy after staining with Hoechst 33258, and the apoptotic cells displayed bright blue due to karyopyknosis and chromatin condensation after treating with Hoechst 33258, and the nuclei of dead cells could not be stained (Yang *et al*., 2012). PC3, Bcap-37, and MGC-803 cells treated with compound **5f** at 5 μM for 12 h were stained with Hoechst 33258. HCPT was used as a positive control at 10 μM for 12 h. The results are shown in Fig. 5.

It can been seen from Fig. 5 that a part of cells with smaller nuclei and condensed staining appeared in the positive control compared with the negative control. After treated with compound **5f**, some cell nuclei became pyknotic (shrunken and dark) or appeared to be highly condensed (brightly stained). These findings once again indicated that compound **5f** could induce apoptosis in tumor cells.

Endonucleases were activated when cells exhibited apoptosis, then DNA was degraded selectively, forming 50–300 kb big fragments, then cleaved in the vicinity of nucleosome and formed DNA fragments of or multiples of 180–200 bp. These DNA fragments could be extracted from cells. The DNA appeared by agarose gel electrophoresis and EB staining (Yuan *et al*., 2011). With HCPT

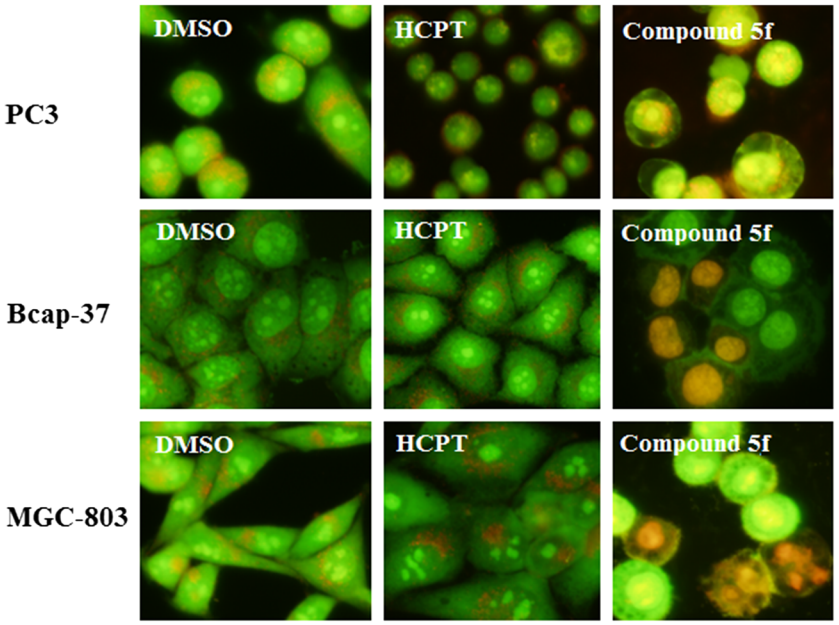

Fig. 4 Nuclei morphological changes during **5f** induced apoptosis in tumor cells detected by AO/EB staining

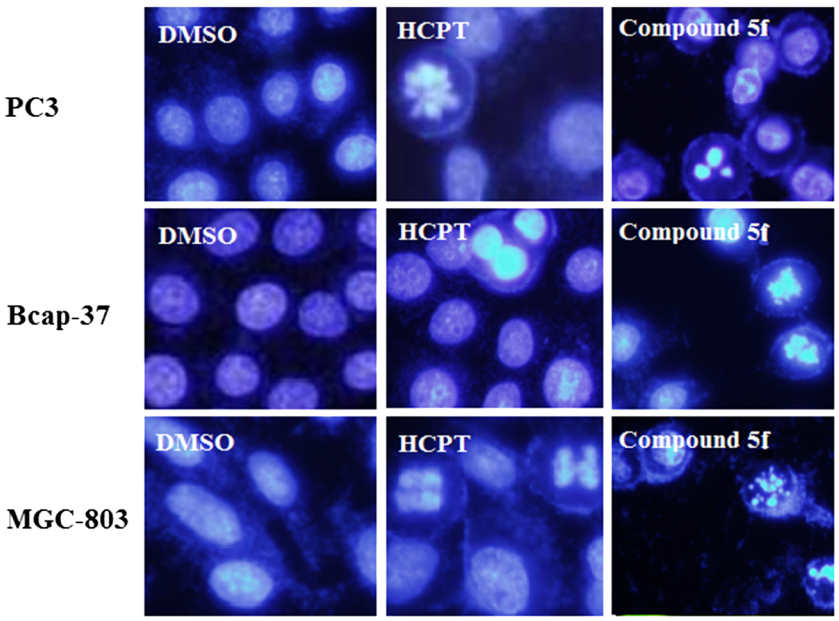

Fig. 5 Nuclei morphological changes during **5f** induced apoptosis in tumor cells detected by Hechst 33258 staining

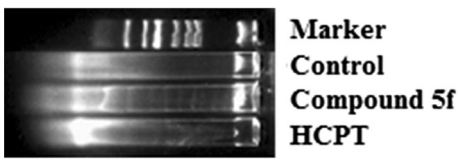

Fig. 6 The DNA ladder of **5f** on MGC-803 cells

used as positive control at 10 μM for 12 h, the compound **5f** induced apoptosis in MGC-803 cells at 5 μM for 12 h, as detected by agarose gel electrophoresis. As shown in Fig. 6, the HCPT and compound **5f** groups appeared as typical DNA Ladder compared with negative group. Therefore, the results indicated that compound **5f** could induce apoptosis in MGC-803 cells.

The apoptosis ratios induced by compound **5f** in tumor cells were quantitatively assessed by FCM. In the early stages of apoptosis, phosphatidylserine was translocated from within the cell membrane to the cell exterior. Annexin V, a calcium-dependent phospholipid-binding protein associated with a high affinity for phosphatidylserine, was used to detect early apoptotic cells. Propidine iodide (PI) is a red fluorescent dye that stains cells with lost their membrane integrity. Cells stained with Annexin V-fluorescein isothiocyanate and PI were classified as necrotic (Q1, Annexin^{-}/PI^{+}), late apoptotic (Q2, Annexin^{+}/PI^{+}),

Table 3 The apoptosis ratios of MGC-803 cells treated with **5f** assessed by flow cytometry

Compound	6 h[a]			12 h			24 h		
	1 μM[b]	5 μM	10 μM	1 μM	5 μM	10 μM	1 μM	5 μM	10 μM
5f (%)	2.4	4.1	6.4	2.8	6.2	10.5	5.3	8.9	27.1
HCPT (%)	1.2	1.8	3.0	2.0	5.8	8.6	4.7	7.6	24.5

[a] Treating time

[b] Agent concentration

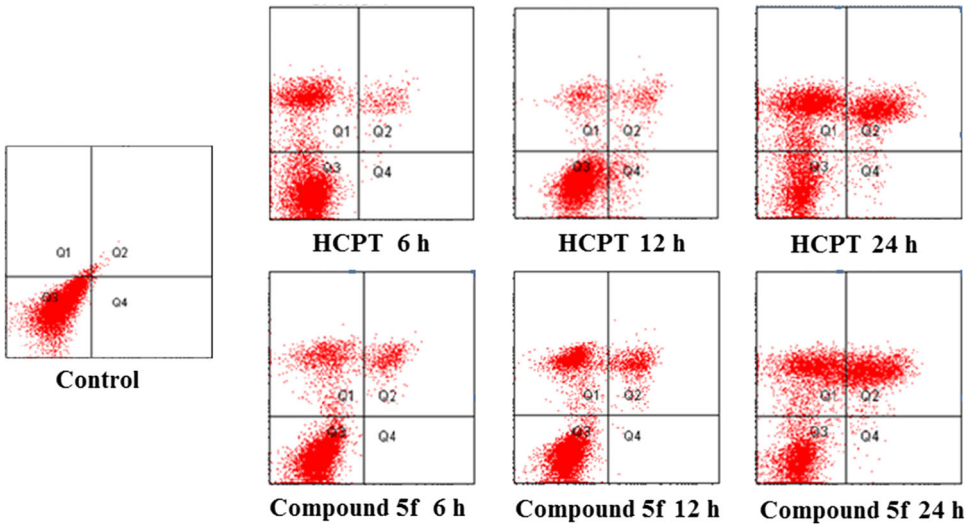

Fig. 7 Flow cytometry analysis for apoptosis inducing activities of **5f** on MGC-803 cells. In the figure, the MGC-803 cells were treated with HCPT and compound **5f** (10 μM) for 6, 12, and 24 h

intact (Q3, Annexin$^-$/PI$^-$), and early apoptotic (Q4, Annexin$^+$/PI$^-$) cells (Yang *et al*., 2013). As shown in Table 3, with HCPT (1, 5, and 10 μM) as positive control, compound **5f** (1, 5, and 10 μM) could induce apoptosis in MGC-803 cells. The highest apoptosis ratio (including the early and late apoptosis ratios) of 27.1 % was obtained after 24 h of treatment at a concentration of 10 μM, and it was markedly higher than that of the positive control HCPT (24.5 % at 10 μM after 24 h of treatment). Furthermore, as shown in Fig. 7, the apoptosis of MGC-803 cells which is treated with compound **5f** increased gradually in a time-dependent manner.

Conclusion

In summary, we have synthesized sixteen novel CC analogs and evaluated for their antitumor activities. Among these new compounds, most of them exhibited good antiproliferative activities against PC3, Bcap-37, and MGC-803 cells. Compound **5f** was found to have the best antitumor activities, with the IC_{50} values of 1.34 ± 0.28, 3.90 ± 0.36, and 0.86 ± 0.44 μM on these three cells, respectively. In addition, subsequent fluorescence staining (AO/EB staining and Hoechst 33258 staining) indicated that the compound could induce apoptosis in PC3, Bcap-37, and MGC-803 cells. And DNA ladder and flow cytometry analysis also revealed that it inhibited the growth of MGC-803 cells via inducing apoptosis, with apoptosis ratio of 27.1 % at 24 h after treatment at 10 μM, higher than the ratio observed for the positive control HCPT (24.5 %). Further studies of the specific mechanisms of these compounds on human malignant tumors are currently underway.

Experimental

General procedures and reagents

^{1}H NMR and ^{13}C NMR were recorded using a JEOL-ECX500 spectrometer at 22 °C, with tetramethylsilane as the internal standard and $CDCl_3$ as the solvent. Elemental analysis was performed with an Elementar Vario-III CHN analyzer. Infrared spectra were recorded on a Bruker VECTOR22 spectrometer in KBr disks. The melting points were determined using an XT-4 digital microscope (melting point apparatus) (Beijing Tech Instrument Co.). Reagents of analytical grade were obtained from Yuda Chemistry Co., Ltd., and used without further purification unless otherwise noted. Column chromatography was performed using silica gel (200–300 mesh) (Qingdao Marine

Chemistry Co., Qingdao, China). Analytical thin-layer chromatography (TLC) was performed on silica gel GF254 (400 mesh).

Synthetic procedures

Quinazolin-4(3H)-one, 8-methyl-quinazolin-4(3*H*)-one, 8-methyl-4-chloroquiazoline, and 4-chloroquiazoline were prepared according to a previously described method (Liu *et al.*, 2004). Intermediate 4-chloroquiazoline was prepared following standard synthetic protocols (Liu *et al.*, 2006). (E)-4-(2-Hydroxyphenyl)-3-butylene-2-one was prepared according to a previously reported (McGookin and Heilbron, 1924).

General synthetic procedures for title compounds

Compounds **5a**–**5n** were synthesized according to Fig. 2. The starting materials were substituted 2-aminobenzoic acid, formamide, salicylaldehyde, and acetone. Substituted *o*-aminobenzoic acid was reacted with formamide for 4.5 h at 140–145 °C to obtain the intermediate 4-quinazolinone **1**. Substituted 4-chloroquinazoline **2** was synthesized via efficient chlorination with use of $SOCl_2$. Intermediates **4a** and **4b** were synthesized starting from the (*E*)-4-(4-hydroxyphenyl)-3-butene-2-one with K_2CO_3 in acetonitrile for 3.5 h at 30–40 °C. Finally, compounds **5a**–**5n** were obtained via condensation of intermediate **4a** or **4b** and substituted aldehydes. IR, ^{1}H NMR, ^{13}C NMR, and elemental analysis data for all the synthesized compounds are reported in the experimental protocols.

*(E)-4-(4-(Quinazolin-4-yloxy)phenyl)but-3-en-2-one (**4a**)*

Yellow powder; mp 97–99 °C; yield: 76.8 %; ESI–MS: 291 $[M+H]^+$; IR (KBr, cm^{-1}) *v*: 1690, 1609, 1578, 1478, 1400, 1354, 1219, 936, 768; ^{1}H NMR (500 MHz, $CDCl_3$) δ: 8.74 (s, 1H, Qu-2-H), 8.33 (d, $J = 2.0$ Hz, 1H, Qu(Quinazolin)-8-H), 7.98 (d, $J = 8.6$ Hz, 1H, Qu-5-H), 7.90 (t, $J = 8.4$ Hz, 1H, Qu-7-H), 7.63–7.65 (m, 3H, Qu-6-H, Ar–CH=, Ar-3-H), 7.51 (d, $J = 16.5$ Hz, 1H,Ar-5-H), 7.29 (d, $J = 8.6$ Hz, 1H, Ar-2,6-H), 6.68 (d, $J = 16.0$ Hz, 1H, Ar–C=CH), 2.37 (s, 3H, $–CH_3$); ^{13}C NMR (125 MHz, $CDCl_3$) δ: 198.3 (C=O), 166.7 (C-4), 154.1 (C-2), 154.0 (C-11), 151.8 (C-9), 142.3 (C-17), 134.4 (C-14), 132.4 (C-13, C-15), 129.8 (C-7), 128.0 (C-8), 127.9 (C-6), 127.4 (C-18), 123.6 (C-12, 16), 122.7(C-5), 116.4 (C-10), 27.8 (CH_3).

*(E)-4-(4-((8-methylquinazolin-4-yl)oxy)phenyl)but-3-en-2-one (**4b**)*

Yellow powder; mp 145–147 °C; yield: 80.6 %; ESI–MS: 305 $[M+H]^+$; IR (KBr, cm^{-1}) *v*: 1665, 1601, 1566, 1487, 1385, 1385, 1211, 972, 777; ^{1}H NMR (500 MHz, $CDCl_3$) δ: 8.81 (s, 1H, Qu-2-H), 8.31(d, $J = 8.5$ Hz, 1H, Qu-5-H), 8.09 (d, $J = 8.6$ Hz, 1H, Qu-7-H), 7.78 (d, $J = 8.6$ Hz, 1H, Ar–CH=), 7.54–7.71 (m, 3H, Ar-2,3,5-H), 7.34 (d, $J = 8.6$ Hz, 1H, Ar-6-H), 6.73 (d, $J = 16.5$ Hz, 1H, ArC=CH), 2.66 (s, 3H, Qu-CH_3), 2.41(s, 3H, $–CH_3$); ^{13}C NMR (125 MHz, $CDCl_3$) δ: 198.4 (C=O), 162.7 (C-4), 153.1 (C-2), 152.7 (C-12), 150.9 (C-9), 142.4 (C-18), 136.5 (C-7), 134.9 (C-8, 15), 129.8 (C-14, 16), 128.6 (C-6), 127.3 (C-19), 123.6 (C-13, 17), 122.7 (C-5), 116.1 (C-10), 27.4 (CH_3), 17.6 (CH_3).

*(1E,4E)-1-(4-fluorophenyl)-5-(4-(quinazolin-4-yloxy)phenyl)penta-1,4-dien-3-one (**5a**)*

Yellow powder; mp 149–151 °C; yield: 56.9 %; ESI–MS: 397 $[M+H]^+$; IR (KBr, cm^{-1}) *v*: 1653, 1620, 1568, 1493, 1335, 1220, 986; ^{1}H NMR (500 MHz, $CDCl_3$) δ: 8.78 (s, 1H, Qu-2-H), 8.42 (d, $J = 8.5$ Hz, 1H, Qu-8-H), 8.30 (d, $J = 8.0$ Hz, 1H, Qu-5-H), 8.22–8.26 (m, 2H, Qu-6,7-H), 8.07 (d, $J = 8.6$ Hz, 1H, Ar–CH=), 7.98 (d, $J = 8.5$ Hz, 1H, F–Ar–CH=), 7.72–7.83 (m, 6H, F–Ar-2,6-H, F–Ar–C=CH, Ar–C=CH, Ar-3,5-H), 7.32 (d, $J = 8.6$ Hz, 2H, F–Ar-3,5-H), 7.20 (d, $J = 16.5$ Hz, 2H, Ar-2-H), 7.06 (d, $J = 16.0$ Hz, 1H, Ar-6-H); ^{13}C NMR (125 MHz, $CDCl_3$) δ: 188.8 (C=O), 166.8 (C-4), 162.6 (C-25), 160.6 (C-2), 154.2 (C-11), 151.9 (C-9), 151.6 (C-21), 136.8 (C-17), 136.1 (C-7), 134.5 (C-14), 131.7 (C-13, 15), 129.4 (C-22), 128.3 (C-23, 27), 128.2 (C-8), 128.1 (C-6), 127.1 (C-20), 126.7 (C-18), 123.6 (C-12, 16), 123.5 (C-5), 116.2 (C-10), 111.5 (C-24, 26); Anal. Calcd for $C_{25}H_{17}FN_2O_2$: C, 75.75; H, 4.32; N, 7.07; Found: C, 75.79; H, 4.71; N, 7.23.

*(1E,4E)-1-(4-chlorophenyl)-5-(4-(quinazolin-4-yloxy)phenyl)penta-1,4-dien-3-one (**5b**)*

Yellow powder; mp 220–222 °C; yield: 59.4 %; ESI–MS: 413 $[M+H]^+$; IR (KBr, cm^{-1}) *v*: 1654, 1595, 1522, 1489, 1385, 1336, 1275, 964; ^{1}H NMR (500 MHz, $CDCl_3$) δ: 8.78 (s, 1H, Qu-2-H), 8.37 (d, $J = 7.5$ Hz, 1H, Qu-8-H), 8.14 (d, $J = 16.5$ Hz, 1H, Cl–Ar–CH=), 8.02 (d, $J = 8.0$ Hz, 1H, Qu-5-H), 7.93 (t, $J = 7.6$ Hz, 1H, Qu-7-H), 7.69–7.79 (m, 5H, Qu-6-H, Ar–CH=, Cl–Ar-3,6-H, Ar-3-H), 7.43 (d, $J = 7.5$ Hz, 1H, Ar-5-H), 7.31–7.35 (m, 4H, Cl–Ar-4,5-H, Cl–Ar–C=CH, Ar–C=CH), 7.12 (d, $J = 16.0$ Hz, 1H, Ar-2-H), 7.03 (d, $J = 16.5$ Hz, 1H, Ar-6-H); ^{13}C NMR (125 MHz, $CDCl_3$) δ: 188.8 (C=O), 166.8 (C-4), 154.2 (C-2), 153.2 (C-11), 151.9 (C-9), 142.7 (C-17), 139.2 (C-21), 134.4 (C-22), 133.1 (C-25), 132.7 (C-14), 131.3 (C-7), 130.0 (C-13, 15), 128.2 (C-23, 27), 128.1 (C-8), 127.9 (C-24, 26), 127.8 (C-6), 127.2 (C-20), 125.1 (C-18), 123.6 (C-12, 16), 122.7 (C-5), 116.3 (C-10); Anal.

Calcd for $C_{25}H_{17}ClN_2O_2$: C, 72.73; H, 4.15; N, 6.97; Found: C, 72.36; H, 4.44; N, 6.56.

*(1E,4E)-1-(2-methoxyphenyl)-5-(4-(quinazolin-4-yloxy)phenyl)penta-1,4-dien-3-one (**5c**)*

Yellow powder; mp 161–163 °C; yield: 45.9 %; ESI–MS: 409 $[M+H]^+$; IR (KBr, cm^{-1}) *v*: 1647, 1618, 1570, 1489, 1337, 1213, 983; ^1H NMR (500 MHz, $CDCl_3$) δ: 8.77 (s, 1H, Qu-2-H), 8.38 (d, $J = 2.5$ Hz, 1H, Qu-8-H), 8.02–8.10 (m, 2H, Qu-5,7-H), 7. 94 (d, $J = 3.6$ Hz, 1H, CH_3O-Ar–CH=), 7.68–7.77 (m, 4H, Qu-6-H, Ar–CH=, CH_3O-Ar-6-H, Ar–C=CH), 7.61 (t, $J = 7.6$ Hz, 1H, CH_3O-Ar-4-H), 7.33–7.38 (m, 3H, Ar-3,5-H,CH_3O-Ar–C=CH), 7.12–7.15 (m, 2H, CH_3O-Ar-3,5-H), 6.93–6.99 (m, 2H, Ar-2,6-H); ^{13}C NMR (125 MHz, $CDCl_3$) δ: 189.5 (C=O), 166.8 (C-4), 158.7 (C-23), 154.2 (C-2), 153.9 (C-11), 151.9 (C-9, 21), 141.8 (C-17), 138.9 (C-27), 134.4 (C-14), 133.1 (C-7), 131.9 (C-13, 15), 128.9 (C-25), 128.1 (C-8), 127.9 (C-6), 126.5 (C-22), 125.6 (C-20), 123.7 (C-18), 123.6 (C-12, 16), 122.6 (C-26), 120.9 (C-5), 115.8 (C-10), 111.3 (C-24), 55.6 (OCH_3);

Anal. Calcd for $C_{26}H_{20}N_2O_3$: C, 76.45; H, 4.94; N, 6.86; Found: C, 76.21; H, 5.24; N, 7.02.

*(1E,4E)-1-(2,4-dichlorophenyl)-5-(4-(quinazolin-4-yloxy)phenyl)penta-1,4-dien-3-one (**5d**)*

Yellow powder; mp 154–156 °C; yield: 65.4 %; ESI–MS: 447 $[M+H]^+$; IR (KBr, cm^{-1}) *v*: 1653, 1616, 1489, 1338, 1217, 906; ^1H NMR (500 MHz, $CDCl_3$) δ: 8.78 (s, 1H, Qu-2-H), 8.38–8.39 (d, $J = 5.0$ Hz, 1H, Qu-8-H), 8.03–8.07 (m, 5H, Qu-5,6,7-H, Cl–Ar–CH=, Ar–CH=), 7.65–7.76 (m, 5H, Cl–Ar-3,5,6-H,Ar-3,5-H), 7.34–7.36 (m, 2H, Cl–Ar–C=CH, Ar–C=CH), 7.10 (d, $J = 15.0$ Hz, 1H, Ar-2-H), 7.03 (d, $J = 15.0$ Hz, 1H, Ar-6-H); ^{13}C NMR (125 MHz, $CDCl_3$) δ: 188.5 (C=O), 166.8 (C-4), 157.1 (C-2), 154.2 (C-11), 153.1 (C-21), 151.9 (C-9), 142.9 (C-17), 137.9 (C-23), 136.6 (C-7), 136.1 (C-14), 134.5 (C-22), 132.7 (C-27), 131.7 (C-13, 15), 130.2 (C-24), 130.0 (C-8), 128.5 (C-6), 128.4 (C-26), 127.9 (C-25), 127.7 (C-20), 125.2 (C-18), 123.6 (C-12, 16), 122.7 (C-5), 116.4 (C-10); Anal. Calcd for $C_{25}H_{16}Cl_2N_2O_2$: C, 67.13; H, 3.61; N, 6.26; Found: C, 67.49; H, 3.45; N, 5.97.

*(1E,4E)-1-(2,5-dimethoxyphenyl)-5-(4-(quinazolin-4-yloxy)phenyl)penta-1,4-dien-3-one (**5e**)*

Yellow powder; mp 146–148 °C; yield: 46.3 %; ESI–MS: 439 $[M+H]^+$; IR (KBr, cm^{-1}) *v*: 1627, 1566, 1520, 1487, 1341, 1217, 983; ^1H NMR (500 MHz, $CDCl_3$) δ: 8.77 (s, 1H, Qu-2-H), 8.38 (d, $J = 8.5$ Hz, 1H, Qu-8-H), 7.95–8.07 (m, 3H, Qu-5,6,7-H), 7.68–7.79 (m, 4H, CH_3O-Ar–CH=, Ar–CH=, Ar-3,5-H), 7.20–7.34 (m, 5H, Ar–C=CH, CH_3O-Ar–C=CH, Ar-2,6-H, CH_3O-Ar-6-H), 6.93 (d, $J = 15.0$ Hz, 1H, CH_3O-Ar-3-H), 6.79 (d, $J = 16.5$ Hz, 1H, CH_3O-Ar-4-H), 3.92 (s, 3H, CH_3O-2-Ar), 3.97 (s, 3H, CH_3O-6-Ar); ^{13}C NMR (125 MHz, $CDCl_3$) δ: 188.7 (C=O), 166.7 (C-4), 155.3 (C-2), 154.2 (C-11, 26), 153.9 (C-21), 151.8 (C-23), 151.0 (C-9), 141.7 (C-17), 134.4 (C-7), 129.8 (C-14), 128.1(C-13, 15), 127.9 (C-8), 126.7 (C-6), 125.5 (C-18), 123.7 (C-20), 122.6 (C-12, 16), 122.5 (C-5), 116.3 (C-22), 116.2 (C-10), 116.1 (C-27), 113.2 (C-24), 112.6 (C-25), 56.2 (OCH_3), 55.9 (OCH_3); Anal. Calcd for $C_{27}H_{22}N_2O_4$: C, 73.96; H, 5.06; N, 6.39; Found: C, 73.65; H, 5.34; N, 6.15.

*(1E,4E)-1-(2-chloro-5-nitrophenyl)-5-(4-(quinazolin-4-yloxy)phenyl)penta-1,4-dien-3-one (**5f**)*

Yellow powder; mp 235–237 °C; yield: 64.7 %; ESI–MS: 458 $[M+H]^+$; IR (KBr, cm^{-1}) *v*: 1653, 1624, 1570, 1522, 1489, 1346, 1217, 906; ^1H NMR (500 MHz, $CDCl_3$) δ: 8.79 (s, 1H, Qu-2-H), 8.59 (s, 1H, Cl–Ar-6-H), 8.38 (d, $J = 8.0$ Hz, 1H, Qu-8-H), 8.18 (d, $J = 6.3$ Hz, 1H, Cl–Ar-4-H), 8.02–8.10 (m, 2H, Qu-5,7-H), 7.94 (t, $J = 7.9$ Hz, 1H, Qu-6-H), 7.62–7.85 (m, 6H, Cl–Ar–CH=Cl–Ar–C=CH, Ar–CH=, Cl–Ar-3-H, Ar-3,5-H), 7.37 (d, $J = 8.6$ Hz, 1H, Ar–C=CH), 7.23 (d, $J = 16.0$ Hz, 1H, Ar-2-H), 7.09 (d, $J = 16.5$ Hz, 1H, Ar-6-H); ^{13}C NMR (125 MHz, $CDCl_3$) δ: 187.8 (C=O), 166.7 (C-4), 154.4 (C-2), 154.1 (C-11), 151.6 (C-9, 21), 146.6 (C-26), 143.6 (C-17), 141.7 (C-23), 134.5 (C-22), 134.0 (C-7), 132.4 (C-13, 15), 131.4 (C-14), 130.2 (C-24), 129.8 (C-8), 128.1 (C-6), 127.9 (C-25), 125.6 (C-20), 125.2 (C-18), 123.6 (C-27), 122.8 (C-12, 16), 122.6 (C-5), 116.4 (C-10); Anal. Calcd for $C_{25}H_{16}ClN_3O_4$: C, 65.58; H, 3.52; N, 9.18; Found: C, 65.55; H, 3.21; N, 9.17.

*(1E,4E)-1-(5-chloro-1,3-dimethyl-1H-pyrazol-4-yl)-5-(4-(quinazolin-4-yloxy)phenyl)penta-1,4-dien-3-one (**5g**)*

Yellow powder; mp 143–145 °C; yield: 57.6 %; ESI–MS: 431 $[M+H]^+$; IR (KBr, cm^{-1}) *v*: 1655, 1618,1587, 1481, 1316, 1219, 987; ^1H NMR (500 MHz, $CDCl_3$, ppm) δ: 8.74 (s, 1H, Qu-2-H), 8.43 (d, $J = 8.0$ Hz, 1H, Qu-8-H), 8.27 (d, $J = 8.5$ Hz, 1H, Qu-5-H), 7.87 (t, $J = 7.4$ Hz, 1H, Qu-7-H), 7.80 (d, $J = 8.5$ Hz, 1H, Ar–CH=), 7.61–7.74 (m, 2H, pyrazole-CH=, Qu-6-H), 7.28–7.51 (m, 3H, Ar-2,3,5-H), 7.28 (d, $J = 8.0$ Hz, 1H, pyrazole-C=CH), 7.09 (d, $J = 16.0$ Hz, 1H, Ar–C=CH), 6.68 (d, $J = 16.5$ Hz, 1H, Ar-6-H), 3.75 (s, 3H, N–CH_3), 2.18 (s, 3H, CH_3); ^{13}C NMR (125 MHz, $CDCl_3$) δ: 187.6 (C=O), 165.8 (C-4), 152.2 (C-2), 150.9 (C-11), 150.4 (C-9, 21), 148.7 (C-26), 141.6 (C-17), 135.9 (C-23), 134.3 (C-7), 132.7 (C-14), 129.2 (C-13, 15), 128.2 (C-20), 128.1 (C-8), 127.9 (C-6), 123.8 (C-8),

123.4 (C-12, 16), 121.9 (C-5), 116.2 (C-10), 112.5 (C-22), 36.3 (CH_3), 14.1 (CH_3); Anal. Calcd for $C_{24}H_{19}ClN_4O_2$: C, 66.90; H, 4.44; N, 13.00; Found: C, 66.71; H, 4.23; N, 13.28.

*(1E,4E)-1-(4-fluorophenyl)-5-(4-((8-methylquinazolin-4-yl)oxy)phenyl)penta-1,4-dien-3-one (**5h**)*

Yellow powder; mp 159–161 °C; yield: 60.5 %; ESI–MS: 411 $[M+H]^+$; IR (KBr, cm^{-1}) *v*: 1668, 1616, 1584, 1479, 1404, 1360, 1220, 984; ^1H NMR (500 MHz, $CDCl_3$) δ: 8.82 (s, 1H, Qu-2-H), 8.22 (d, $J = 8.0$ Hz, 1H, Qu-5-H), 7.69–7.78 (m, 5H, Qu-6,7-H, Ar–CH=, F–Ar–CH=, F–Ar-2-H), 7.57–7.62 (m, 3H, F–Ar-6-H, Ar-3,5-H), 7.33 (d, $J = 7.6$ Hz, 2H, F–Ar-3,5-H), 6.99–7.11 (m, 4H, F–Ar–C=CH, Ar–C=CH, Ar-2,6-H), 2.77 (s, 1H, CH_3); ^{13}C NMR (125 MHz, $CDCl_3$) δ: 189.3 (C=O), 167.1 (C-4), 161.3 (C-26), 154.3 (C-2), 153.0 (C-12), 151.2 (C-9), 143.6 (C-18), 142.3 (C-22), 136.6 (C-7), 134.8 (C-8), 133.3 (C-15), 132.6 (C-24, 28), 129.9 (C-23), 129.6 (C-14, 16), 129.4 (C-6), 127.4 (C-19), 125.7 (C-21), 122.7 (C-13, 17), 121.3 (C-5), 116.2 (C-10), 110.6 (C-25, 27), 17.8 (CH_3); Anal. Calcd for $C_{26}H_{19}FN_2O_2$: C, 76.08; H, 4.67; N, 6.83; Found: C, 76.40; H, 4.43; N, 7.12.

*(1E,4E)-1-(4-chlorophenyl)-5-(4-((8-methylquinazolin-4-yl)oxy)phenyl)penta-1,4-dien-3-one (**5i**)*

Yellow powder; mp 188–190 °C; yield: 51.5 %; ESI–MS: 427 $[M+H]^+$; IR (KBr, cm^{-1}) *v*: 1653, 1620, 1581, 1481, 1359, 1223, 984; ^1H NMR (500 MHz, $CDCl_3$) δ: 8.82 (s, 1H, Qu-2-H), 8.21–8.23 (d, $J = 10.0$ Hz, 1H, Cl–Ar–CH=), 7.68–7.79 (m, 4H, Qu-5,6,7-H, Ar–CH=), 7.54–7.58 (m, 4H, Cl–Ar-2,3,5,6-H), 7.34–7.57 (m, 4H, Ar-3, 5-H, Cl–Ar–C=CH, Ar–C=CH), 7.04–7.07 (d, $J = 10.0$ Hz, 2H, Ar-2,6-H), 2.77 (s, 3H, CH_3); ^{13}C NMR (125 MHz, $CDCl_3$) δ: 188.6 (C=O), 167.0 (C-4), 154.3 (C-2), 153.1 (C-12), 151.0 (C-9), 142.6 (C-18), 142.1 (C-22), 136.5 (C-7), 134.5 (C-8), 133.3 (C-26), 132.6 (C-23), 129.9 (C-15), 129.6 (C-14, 16), 129.4 (C-24, 28), 127.4 (C-25, 27), 125.9 (C-6), 123.4 (C-21), 122.7 (C-19), 121.2 (C-13, 17), 120.4 (C-5), 116.3 (C-10), 17.7 (CH_3); Anal. Calcd for $C_{26}H_{19}ClN_2O_2$: C, 73.15; H, 4.49; N, 6.56; Found: C, 72.99; H, 4.81; N, 6.77.

*(1E,4E)-1-(2-methoxyphenyl)-5-(4-((8-methylquinazolin-4-yl)oxy)phenyl)penta-1,4-dien-3-one (**5j**)*

Yellow powder; mp 156–158 °C; yield: 52.6 %; ESI–MS: 423 $[M+H]^+$; IR (KBr, cm^{-1}) *v*: 1647, 1616, 1582, 1481, 1400,1356, 1219, 989; ^1H NMR (500 MHz, $CDCl_3$) δ: 8.81 (s, 1H, Qu-2-H), 8.21 (d, $J = 7.0$ Hz, 1H, CH_3O-Ar–CH=), 8.07 (d, $J = 16.6$ Hz, 1H, Ar–CH=), 7.74–7.77 (m, 4H, Qu-5,6,7-H, CH_3O-Ar-6-H), 7.55–7.61 (m, 2H, Ar-3,5-H), 7.31–7.37 (m, 3H, CH_3O-Ar-4-H, CH_3O-Ar–C=CH, Ar–C=CH), 7.12–7.19 (m, 2H, CH_3O-Ar-3,5-H), 6.95 (d, $J = 16.5$ Hz, 2H, Ar-2,6-H), 3.86 (s, 3H. OCH_3), 2.77 (s, 3H. CH_3); ^{13}C NMR (125 MHz, $CDCl_3$) δ: 189.5 (C=O), 167.1 (C-4), 158.7 (C-24), 154.2 (C-2), 154.1 (C-12), 153.2 (C-22), 150.9 (C-9), 141.9 (C-18), 138.9 (C-7), 136.5 (C-28), 134.47 (C-8), 131.9 (C-15), 129.9 (C-14, 16), 129.7 (C-26), 128.9 (C-6), 127.4 (C-23), 126.5 (C-19), 125.6 (C-21), 123.8 (C-13, 17), 122.6 (C-27), 121.2 (C-5), 120.9 (C-10), 111.3 (C-25), 55.6 (OCH_3), 17.7 (CH_3); Anal. Calcd for $C_{27}H_{22}N_2O_3$: C, 76.76; H, 5.25; N, 6.63; Found: C, 76.60; H, 5.16; N, 6.52.

*(1E,4E)-1-(2,4-dichlorophenyl)-5-(4-((8-methylquinazolin-4-yl)oxy)phenyl)penta-1,4-dien-3-one (**5k**)*

Yellow powder; mp 203–205 °C; yield: 62.5 %; ESI–MS: 461 $[M+H]^+$; IR (KBr, cm^{-1}) ν: 1653, 1618, 1576,1506, 1477, 1400,1356, 1221, 934; ^1H NMR (500 MHz, $CDCl_3$) δ: 8.82 (s, 1H, Qu-2-H), 8.22 (d, $J = 8.0$ Hz, 1H, Cl–Ar–CH=), 8.04 (d, $J = 16.0$ Hz, 1H, Ar–CH=), 7.73–7.79 (m, 4H, Cl–Ar-3-H, Qu-5,6,7-H), 7.65 (d, $J = 8.6$ Hz, 1H, Cl–Ar-6-H), 7.57 (d, $J = 8.6$, Hz, 1H, Cl–Ar-5-H), 7.46 (d, $J = 2.4$ Hz, 1H, Ar–C=CH), 7.28–7.33 (m, 3H, Cl–Ar–C=CH, Ar-3,5-H), 7.07 (d, $J = 16.0$ Hz, 1H, Ar-2-H), 7.02 (d, $J = 16.0$ Hz, 1H, Ar-6-H), 2.77 (s, 3H, CH_3); ^{13}C NMR (125 MHz, $CDCl_3$) δ: 188.5 (C=O), 167.0 (C-4), 154.4 (C-2), 153.1 (C-12), 151.0 (C-9, 22), 142.9 (C-18), 137.9 (C-24), 136.6 (C-7), 136.5 (C-8), 134.5 (C-15), 132.6 (C-23), 131.7 (C-28), 130.2 (C-14, 16), 130.0 (C-25), 128.5 (C-6), 128.4 (C-27), 127.7 (C-26), 127.4 (C-21), 125.1 (C-19), 122.7 (C-13, 17), 121.2 (C-5), 116.3 (C-10), 17.7 (CH_3); Anal. Calcd for $C_{26}H_{18}Cl_2N_2O_2$: C, 67.69; H, 3.93; N, 6.07; Found: 67.92; H, 3.56; N, 5.79.

*(1E,4E)-1-(2,5-dimethoxyphenyl)-5-(4-((8-methylquinazolin-4-yl)oxy)phenyl)penta-1,4-dien-3-one (**5l**)*

Yellow powder; mp 171–173 °C; yield: 53.4 %; ESI–MS: 453 $[M+H]^+$; IR (KBr, cm^{-1}) *v*: 1658, 1616, 1576,1506, 1478, 1356, 1220, 983; ^1H NMR (500 MHz, $CDCl_3$,) δ: 8.83 (s, 1H, Qu-2-H), 8.23 (d, $J = 8.0$ Hz, 1H, CH_3O-Ar–CH=), 8.05 (d, $J = 8.5$ Hz, 1H, Ar–CH=), 7.74–7.78 (m, 4H, Ar-3-H, Qu-5,6,7-H), 7.57 (d, $J = 7.5$ Hz, 1H, Ar-5-H), 7.30–7.34 (m, 2H, CH_3O-Ar–CH=, Ar–CH=), 7.06–7.15 (m, 3H, Ar-2,6-H, CH_3O-Ar-6-H), 6.87–6.93 (m, 2H, CH_3O-Ar-3,4-H), 3.86 (s, 6H, $2CH_3O$), 2.77 (s, 3H, CH_3); ^{13}C NMR (125 MHz, $CDCl_3$) δ: 189.4 (C=O), 167.1 (C-4), 155.2 (C-2), 154.1 (C-12), 153.6 (C-27), 153.2 (C-22), 150.3 (C-24), 148.4 (C-9), 141.9 (C-18), 138.6 (C-7), 136.5 (C-8), 129.9 (C-15), 127.4 (C-14, 16), 126.7 (C-6),

125.4 (C-19), 124.4 (C-21), 122.6 (C-13, 17), 121.2 (C-5), 117.6 (C-10, 23), 113.2 (C-25), 112.6 (C-26, 28), 56.2 (OCH_3), 55.9 (OCH_3), 17.7 (CH_3); Anal. Calcd for $C_{28}H_{24}N_2O_4$: C, 74.32; H, 5.35; N, 6.19; Found: C, 74.20; H, 5.43; N, 6.08.

*(1E,4E)-1-(2-chloro-5-nitrophenyl)-5-(4-((8-methylquinazolin-4-yl)oxy)phenyl)penta-1,4-dien-3-one (**5m**)*

Yellow powder; mp 214–216 °C; yield: 62.5 %; ESI–MS: 472 $[M+H]^+$; IR (KBr, cm^{-1}) *v*: 1653, 1626, 1579, 1479, 1402,1348, 1221, 1165, 1111, 979, 766; ^1H NMR (500 MHz, $CDCl_3$) δ: 8.83 (s, 1H, Qu-2-H), 8.60 (s, 1H, Cl–Ar-6-H), 8.08–8.23 (m, 4H, Cl–Ar-4-H, Qu-5,6,7-H), 7.76–7.85 (m, 4H, Cl–Ar-3-H, Ar–CH=, Cl–Ar–CH=, Cl–Ar–C=CH), 7.57–7.65 (m, 2H, Ar-3,5-H), 7.36 (d, $J = 8.5$ Hz, 1H, Ar–C=CH), 7.23 (d, $J = 16.5$ Hz, 1H, Ar-2-H), 7.08 (d, $J = 16.5$ Hz, 1H, Ar-6-H), 2.77 (s, 3H, CH_3); ^{13}C NMR (125 MHz, $CDCl_3$) δ: 187.8 (C=O), 167.0 (C-4), 154.6 (C-2), 153.1 (C-12), 151.0 (C-22), 146.8 (C-9), 144.2 (C-27), 143.7 (C-18), 141.8 (C-24), 136.6 (C-7), 136.6 (C-8), 134.5 (C-23), 131.4 (C-15), 130.2 (C-14, 16), 130.1 (C-6), 129.8 (C-25), 127.4 (C-26), 125.5 (C-21), 125.2 (C-19), 122.8 (C-28), 122.6 (C-13, 17), 121.2 (C-5), 116.3 (C-10), 17.8 (CH_3); Anal. Calcd for $C_{26}H_{18}ClN_3O_4$: C, 66.18; H, 3.84; N, 8.90; Found: C, 66.42; H, 3.78; N, 8.65.

*(1E,4E)-1-(5-chloro-1,3-dimethyl-1H-pyrazol-4-yl)-5-(4-((8-methylquinazolin-4-yl)oxy) phenyl)penta-1,4-dien-3-one (**5n**)*

Yellow powder; mp 202–204 °C; yield: 62.3 %; ESI–MS: 445 $[M+H]^+$; IR (KBr, cm^{-1}) *v*: 1651, 1616, 1582, 1479, 1359, 1223, 982; ^1H NMR (500 MHz, $CDCl_3$) δ: 8.82 (s, 1H, Qu-2-H), 8.21 (d, $J = 10.0$ Hz, 1H, pyrazole-CH=), 7.72–7.78 (m, 3H, Qu-5,6,7-H), 7.55–7.63 (m, 3H, Ph-3-H, Ar–CH=, pyrazole-C=CH), 7.31–7.33 (m, 2H, Ar–C=CH,Ar-5-H), 6.96–7.04 (m, 2H, Ar-2,6-H), 2.39 (s, 3H, Qu-CH_3), 2.77 (s, 3H, pyrazole-CH_3), 3.82 (s, 3H, N–CH_3); ^{13}C NMR (125 MHz, $CDCl_3$) δ: 188.7 (C=O), 167.1 (C-4), 154.2 (C-2), 153.1 (C-12), 150.9 (C-9, 22), 148.9 (C-27), 141.9 (C-18), 136.5 (C-7), 134.5 (C-8), 132.8 (C-24), 129.9 (C-15), 129.2 (C-21), 127.4 (C-14, 16), 126.0 (C-6), 123.5 (C-19), 122.6 (C-13, 17), 121.2 (C-5), 116.3 (C-10), 112.5 (C-23), 36.3 (CH_3), 17.7 (CH_3), 14.2 (CH_3); Anal. Calcd for $C_{25}H_{21}ClN_4O_2$: C, 67.49; H, 4.76; N, 12.59; Found: C, 67.24; H, 4.98; N, 12.42.

Cell lines and culture

PC3, Bcap-37, MGC-803, and NIH3T3 cell lines were obtained from the Institute of Biochemistry and Cell Biology, China Academy of Science. PC3 is prostate cancer cell line; Bcap-37 is breast cancer cell line; MGC-803 is gastric cancer cell line, and NIH3T3 is mouse embryo fibroblast cell line. The entire cancer cell lines were maintained in the RPMI 1640 medium, whereas the NIH3T3 cell line was maintained in DMEM medium. They were supplemented with 10 % heat-inactivated fetal bovine serum (FBS). All cell lines were maintained at 37 °C in a humidified 5 % carbon dioxide and 95 % air incubator.

MTT assays

All tested compounds were dissolved in DMSO (1-100 μM solution) and subsequently diluted in the culture medium before treatment of the cultured cells. Tested cells were maintained in 96-well plates at a density 2×10^3 cells/well/100 μL of the proper culture medium and treated with the compounds at 1 to 100 μM for 72 h. In parallel, the cells treated with 0.1 % DMSO served as control. A MTT assay (Roche Molecular Biochemicals, 1465-007) was performed 30 h later according to the instructions provided by Roche. This assay was based on the cellular cleavage of MTT into formazane which is soluble in cell culture medium. Any absorbance caused by formazan was measured at 595 nm with a microplate reader (BIO-RAD, model 680), which is directly proportional to the number of living cells in culture. The experiment was performed in triplicate.

AO/EB staining

Six coverslips were first soaked in 75 % alcohol for 6 h and then put into 6 well plates and dried by alcohol lamp; MGC-803 cell suspension (4 mL) was digested and mixed steadily in a centrifuge tube (15 mL). Then 800 μL cell suspensions to per coverslips, 6 well plates were put into incubator. Add 1,200 μL RPMI 1640 culture medium containing 10 %FBS to each well after the cells, cultivate cells continuatively. Add test compounds to 6 well plates when the cells grow to 80 %. The cells were observed after add drug. The cells can be stain when cells morphology changed, add 20 μL stains to glass slide, coverslips in 6 wells plate were covered the surface of stains. The cells were observed and photographed by fluorescence microscope.

Hoechst 33258 staining

The procedures of inoculating well plates and adding drugs are same with AO/EB staining. 0.5 mL fixative solution was added into each well; cells were fixed for 10 min. The wells were washed twice (3 min/once) with 1 × PBS after drain fixative solution. 0.5 mL Hoechst 33258 staining solution was added into each well; the cells were stained for

5 min on shaking table. Then the wells were washed twice (3 min/once) with 1× PBS after staining. Later, coverslips having cells were covered the glass slide; the cells were detected by the violet ray of fluorescence microscope.

DNA ladder

Detect apoptosis by DNA Ladder. The exponential phase of growth MGC-803 cells were inoculated on Petri dish which diameter was 10 cm. The compounds were added into the cells for inducing apoptosis when the cells grow to 80 %. Scraped the cells from culture plate and centrifuged at 2,000 rpm for 2 min after 72 h. Discarded the supernatant and collected the cells, then DNA was extracted with DNA Extraction Kit.

The supernatants were electrophoresed on a 2 % agarose gel at 120 V pressure for 30 min. The results were observed by gel imaging system after electrophoresis.

Flow cytometry analysis

Prepared MGC-803 cells (1×10^6/mL) were washed twice with cold PBS and then resuspended gently in 500 μL binding buffer. Then the cells were stained in 5 μL Annexin V-FITC and shaked well. 5 μL PI was added to these cells and incubated for 20 min in a dark place, analyzed by FACS.

Statistical analysis

All statistical analysis were performed using SPSS 10.0, and the data were analyzed using one-way ANOVA. The mean separations were performed using the least significant difference method. Each experiment was performed in triplicate, and all experiments were run at least three times and yielded similar results. Measurements from all the replicates were combined, and the treatment effects were analyzed.

Acknowledgments The authors wish to thank the Guizhou Province Production Technology & Innovation Capacity Building for Fine Fruits (No. 20104009) and the Science and Technology Major Specialized Projects for "Significant New Drugs Creation" of the 12th 5-year Plan (2012ZX09101231-004) for the financial support.

Conflict of interest None.

References

Almanaa TN, Geusz ME, Jamasbi RJ (2012) Effects of curcumin on stem-like cells in human esophageal squamous carcinoma cell lines. BMC Complement Altern Med 12:195. doi:10.1186/1472-6882-12-195

Archana P, Sathishkumar P, Bharahi N (2011) In silico docking analysis of curcumin-an inhibitor for obesity. Int J Pharm Bio Sci 4:224–235

Bachmeier BE, Mirisola V, Romeo F, Generoso L, Esposito A, Dell'eva R, Blengio F, Killian PH, Albini A, Pfeffer U (2010) Reference profile correlation reveals estrogen-like trancriptional activity of curcumin. Cell Physiol Biochem 26:471–482

Chainani-Wu N (2003) Safety and anti-inflammatory activity of curcumin: a component of tumeric (Curcuma longa). J Altern Complement Med 9:161–168

Fei B, Chi AL, Weng Y (2013) Hydroxycamptothecin induces apoptosis and inhibits tumor growth in colon cancer by the downregulation of survivin and XIAP expression. World J Surg Oncol 11:120. doi:10.1186/1477-7819-11-120

Jayaprakasha GK, Rao LJ, Sakariah KK (2006) Antioxidant activities of curcumin, demethoxycurcumin and bisdemethoxycurcumin. Food Chem 4:720–724

Kasibhatla S, Amarante-Mendes GP, Finucane D, Brunner T, Bossy-Wetzel E, Green DR (2006) Acridine orange/ethidium bromide (AO/EB) staining to detect apoptosis. CSH Protoc. doi:10.1101/pdb.prot4493

Khanna S, Park HA, Sen CK, Golakoti T, Sengupta K, Venkateswarlu S, Roy S (2009) Neuroprotective and anti-inflammatory properties of a novel demethylated curcuminoid. Antioxid Redox Signal 11:449–468. doi:10.1089/ARS.2008.2230

Kohli K, Ali J, Ansari MJ, Raheman Z (2005) Curcumin: a natural anti-inflammatory agent. Indian J Pharmacol 3:141–147

Lee JY, Lee YM, Chang GC, Yu SL, Hsieh WY, Chen JJ, Chen HW, Yang PC (2011) Curcumin induces EGFR degradation in lung adenocarcinoma and modulates p38 activation in intestine: the versatile adjuvant for gefitinib therapy. PLoS One 6:e23756

Lin CL, Lin JK (2008) Curcumin: a potential cancer chemopreventive agent through suppressing NF-κB signaling. J Cancer Mol 4:11–16

Liu G, Song BA, Sang WJ, Yang S, Jin LH, Ding X (2004) Chin J Org Chem 10:1296–1299

Liu G, Yang S, Song BA, Xue W, Hu DY, Jin LH, Lu P (2006) Microwave assisted synthesis of *N*-arylheterocyclic substituted-4-aminoquinazoline derivatives. Molecules 11:272–278

McGookin A, Heilbron IM (1924) CCLXXV.-The isomerism of the styryl alkyl ketones. Part I. The isomerism of 2-hydroxystyryl methyl ketone. J Chem Soc Trans 125:2099–2105

Menon VP, Sudheer AR (2007) Antioxidant and anti-inflammatory properties of curcumin. Adv Exp Med Biol 595:105–125

Ravindran J, Prasad S, Aggarwal BB (2009) Curcumin and cancer cells: how many ways can curry kill tumor cells selectively? AAPS J 11:495–510. doi:10.1208/s12248-009-9128-x

Ringman JM, Frautschy SA, Cole GM, Masterman DL, Cummings JL (2005) A potential role of the curry spice curcumin in Alzheimer's disease. Curr Alzheimer Res 2:131–136

Sa G, Das T (2008) Anti-cancer effects of curcumin: cycle of life and death. Cell Div 3:14

Senft C, Polacin M, Priester M, Seifert V, Kögel D, Weissenberger J (2010) The nontoxic natural compound curcumin exerts anti-proliferative, anti-migratory, and anti-invasive properties against malignant gliomas. BMC Cancer 10:491

Shibata H, Yamakoshi H, Sato A, Ohori H, Kakudo Y, Kudo C, Takahashi Y, Watanabe M, Takano H, Ishioka C, Noda T, Iwabuchi Y (2009) Newly synthesized curcumin analog has improved potential to prevent colorectal carcinogenesis in vivo. Cancer Sci 100:956–960

Shukla PK, Khanna VK, Ali MM, Khan MY, Srimal RC (2008) Anti-ischemic effect of curcumin in rat brain. Neurochem Res 33:1036–1043

Sukardiman H, Widyawaruyanti A, Sismindari, Zaini NC (2007) Apoptosis inducing effect of andrographolide on TD-47 human breast cancer cell line. Afr J Tradit Complement Altern Med 4:345–351

Wilken R, Veena MS, Wang MB, Srivatsan ES (2011) Curcumin: a review of anti-cancer properties and therapeutic activity in head and neck squamous cell carcinoma. Mol Cancer 10:12

Wu J, Yi WS, Jin LH, Hu DY, Song BA (2012) Antiproliferative and cell apoptosis-inducing activities of compounds from *Buddleja davidii* in MGC-803 cells. Cell Div 7:20

Yamakoshi H, Ohori H, Kudo C, Sato A, Kanoh N, Ishioka C, Shibata H, Iwabuchi Y (2010) Structure-activity relationship of C5-curcuminoids and synthesis of their molecular probes thereof. Bioorg Med Chem 18:1083–1092

Yang S, Liang N, Li H, Xue W, Hu D, Jin L, Zhao Q, Yang S (2012) Design, synthesis and biological evaluation of novel betulinic acid derivatives. Chem Cent J 6:141

Yang S, Liu M, Liang N, Zhao Q, Zhang Y, Xue W, Yang S (2013) Discovery and antitumor activities of constituents from *Cyrtomium fortumei* (J.) Smith rhizomes. Chem Cent J 7:24

Yuan K, Song B, Jin L, Xu S, Xu X, Yang S (2011) Synthesis and biological evaluation of novel 1-aryl, 5(phenoxy-substituted)aryl-1,4-pentadien-3-one derivatives. Med Chem Commun 2:585–589

Zahidah AF, Faizah O, Aqilah N, Anna KT (2012) Curcumin as an anti-arthritic agent in collagen-induced arthritic sprague-dawley rats. Sains Malays 41:591–595

Zhai DD, Supaibulwatana K, Zhong JJ (2010) Inhibition of tumor cell proliferation and induction of apoptosis in human lung carcinoma 95-D cells by a new sesquiterpene from hairy root cultures of Artemisia annua. Phytomedicine 17:856–861